

# Materials design in the performance of all-ceramic crowns<sup>☆</sup>

Brian R. Lawn<sup>a,\*</sup>, Antonia Pajares<sup>a,1</sup>, Yu Zhang<sup>a,2</sup>, Yan Deng<sup>a,3</sup>, Mariano A. Polack<sup>a</sup>,  
Isabel K. Lloyd<sup>b</sup>, E. Dianne Rekow<sup>c,d</sup>, Van P. Thompson<sup>c,e</sup>

<sup>a</sup> Materials Science and Engineering Laboratory, National Institute of Standards and Technology, Building 301, Shipping & Receiving, Gaithersburg, MD 20899-8500, USA

<sup>b</sup> Department of Materials Science and Engineering, University of Maryland, College Park, MD 20742-2115, USA

<sup>c</sup> New York University College of Dentistry, 345 East 24th Street, New York, NY 10010, USA

<sup>d</sup> Division of Basic Sciences, New York University College of Dentistry, 345 East 24th Street, New York, NY 10010, USA

<sup>e</sup> Department of Biomaterials and Biomimetics, New York University College of Dentistry, 345 East 24th Street, New York, NY 10010, USA

Received 12 May 2003; accepted 4 September 2003

## Abstract

Results from a systematic study of damage in material structures representing the basic elements of dental crowns are reported. Tests are made on model flat-layer specimens fabricated from various dental ceramic combinations bonded to dentin-like polymer substrates, in bilayer (ceramic/polymer) and trilayer (ceramic/ceramic/polymer) configurations. The specimens are loaded at their top surfaces with spherical indenters, in simulation of occlusal function. The onset of fracture is observed in situ using a video camera system mounted beneath the transparent polymer substrate. Critical loads to induce fracture and deformation at the ceramic top and bottom surfaces are measured as functions of layer thickness and contact duration. Radial cracking at the ceramic undersurface occurs at relatively low loads, especially in thinner layers. Fracture mechanics relations are used to confirm the experimental data trends, and to provide explicit dependencies of critical loads in terms of key variables: *material*—elastic modulus, hardness, strength and toughness; *geometric*—layer thicknesses and contact radius. Tougher, harder and (especially) stronger materials show superior damage resistance. Critical loads depend strongly (quadratically) on crown net thickness. The analytic relations provide a sound basis for the materials design of next-generation dental crowns.

Published by Elsevier Ltd.

**Keywords:** Dental ceramics; Crowns; Materials design; Plasticity; Radial cracks

## 1. Introduction

Ceramics are replacing metals as materials of choice in dental crowns [1], as well as in other biomechanical prostheses (e.g., hip prostheses) [2]. Apart from improved aesthetics, ceramics promise superior biocompatibility and inertness. However, clinical experience

indicates that all-ceramic crowns are not as durable as their porcelain-fused-to-metal counterparts, particularly on molar teeth—ceramics are limited by their brittleness [3–11]. In the 1980s and 1990s, crowns fabricated as enamel-like monoliths from micaceous glass-ceramics (Dicor, Dentsply/Caulk, Milford, DE) and high leucite porcelains (IPS Empress, Ivoclar, Schaan, Lichtenstein) were introduced, but showed unacceptably high failure rates [7,11]. Subsequent crown design has focused on retention of porcelain as an aesthetic veneer but with much stronger alumina-based ceramics, either glass-infiltrated (InCeram, Vita Zahnfabrik, Bad Säckingen, Germany) or (more recently) pure and dense (Procera, Nobel Biocare, Göteborg, Sweden), as supporting cores. Although alumina-based crowns continue to replace metal-based crowns, failure rates remain an issue [10,12]. Lifetime data on crowns fabricated with the latest, ultra-strong core ceramics, e.g. yttria-stabilized

<sup>☆</sup> Information of product names and suppliers in this paper is not to imply endorsement by NIST.

\*Corresponding author. Tel.: +1-301-975-5775; fax: +1-301-975-5012.

E-mail address: [brian.lawn@nist.gov](mailto:brian.lawn@nist.gov) (B.R. Lawn).

<sup>1</sup> On leave from Departamento de Física, Facultad de Ciencias, Universidad de Extremadura, 06071 Badajoz, Spain.

<sup>2</sup> On leave from New York University College of Dentistry, 345 East 24th Street, New York, NY 10010, USA.

<sup>3</sup> Ph.D. program, Department of Materials and Nuclear Engineering, University of Maryland College Park, MD 20742-2115, College Park, MD 20742-2115, USA.

zirconia (Y-TZP) and alumina-matrix composites (AMC) [2], have yet to be documented.

Clinically, bulk fractures are the reported cause of all-ceramic crown failure whether the crown is a monolith or a layered structure [13]. Failure generally does not ensue from damage at the occlusal surface (though some cumulative damage may occur at wear facets), but rather from subsurface radial cracks at the cementation interface [1,14]. The radial cracks are initially contained within the inner core layer, but subsequently propagate to the core boundaries, ultimately causing irretrievable failure. This raises an interesting question—if the ceramic core materials are so strong, why do the cracks not originate in the weak outer porcelain? Porcelain failures do seem to occur preferentially in metal-backed crowns, although there is some indication that such failures may be preceded by plasticity in the ductile metal [15]. What then, are the important material parameters that govern these failure modes in crown structures, and how may they be optimized? As early as 1983, McLean argued intuitively that layered all-ceramic crowns should perform well if the core fracture strength were to exceed the yield strength of base metal alloys (about 400–500 MPa for gold) [16]. But until now there have been few systematic attempts to test this assertion [1,14]. Studies in the dental community continue to be largely governed by methodologies of retrieval analysis and clinical trial.

A principal objective of our investigation is to establish critical conditions for initiation of lifetime-limiting damage in ceramic-based crown-like layer structures. Controlled indentation testing with spheres on flat-layer specimens is used to simulate the basic elements of occlusal loading. While basic, the test procedure is not restrictive—once the materials aspects are understood, complicating factors such as crown geometry, complex chewing motion, role of dental cement, etc. may be added step-by-step into a complete description. *Post-mortem* studies on specimens cross-sectioned through the indentation sites have identified a variety of competing fracture and deformation modes at the top (occlusal) surfaces and crown/substrate (cementation) interfaces, each with the potential to cause damage accumulation and subsequent failure [17–20]. These studies have confirmed that damage occurs when the stress intensity in the layer structure exceeds certain limits—fracture from tensile stresses, yield from shear stresses. Common modes in all-ceramic layer systems are shown schematically in Fig. 1—others are possible and will be discussed later. Interestingly, delamination at the interlayer interfaces is not generally a primary fracture mode, except perhaps in extensive cyclic conditions and/or when one of the crown layers undergoes plastic yield.

In this paper we summarize the results of studies on model layer structures in which the various damage

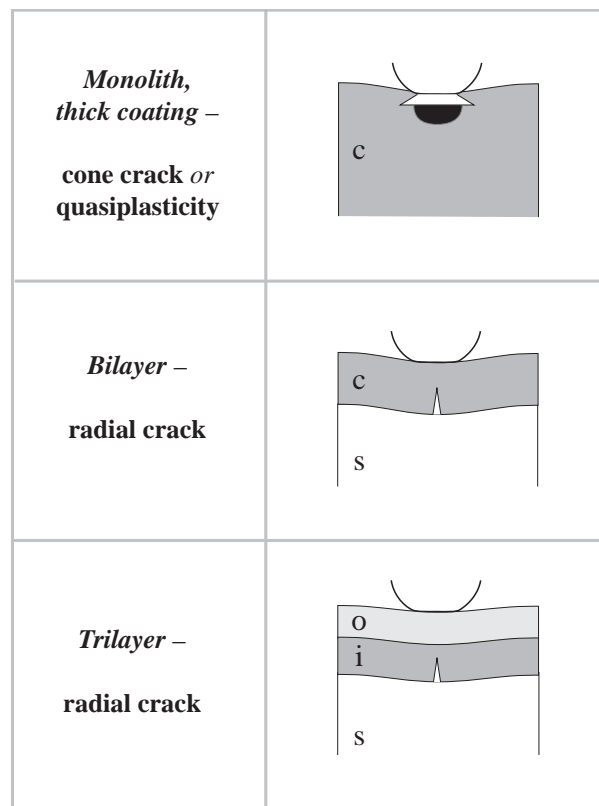


Fig. 1. Schematic of ceramic layers c (bilayers), o and i (trilayers) on compliant substrates s. Common damage modes from occlusal-like contacts indicated: surface cone cracks and quasiplastic yield zone at top surface; radial cracks at ceramic bottom surfaces.

modes can be observed and quantified in situ. Such observations confirm radial cracking as a primary source of failure in all-ceramic crown-like structures, and facilitate the derivation of explicit analytic relations expressing critical loads for initiation of this and other damage modes in terms of materials properties and layer thicknesses.

## 2. Methods and materials

Crown-like layer structures were constructed from dental ceramics bonded to dentin-like transparent polycarbonate bases [21–23]. Basic properties of the relevant materials are listed in Table 1: Young's modulus (resistance to elastic deformation), hardness (resistance to plastic deformation), strength (resistance to crack initiation) and toughness (resistance to crack propagation). The ceramics were supplied by the manufacturers as plates with minimum lateral dimension 15 mm, ground flat and parallel and surface-polished with 1  $\mu$ m diamond paste. In the case of bilayers, monolithic ceramic plates were directly bonded to the substrates using transparent epoxy adhesive as cement. For trilayers, a porcelain-like soda-lime glass

Table 1  
Properties of dental materials

| Material                       | Name        | Supplier          | Modulus $E$<br>(GPa) | Hardness $H$<br>(GPa) | Toughness $T$<br>(MPa m <sup>1/2</sup> ) | Strength $S$<br>(MPa) |
|--------------------------------|-------------|-------------------|----------------------|-----------------------|--|-----------------------|
| <i>Core ceramic</i>            |             |                   |                      |                       |  |                       |
| Glass-ceramic                  | Empress II  | Ivoclar           | 104                  | 5.5                   | 2.9                                      | 420                   |
| Alumina (infiltr)              | InCeram     | Vita Zahnfabrik   | 270                  | 12.3                  | 3.0                                      | 550                   |
| Zirconia (infiltr)             | InCeram     | Vita Zahnfabrik   | 245                  | 13.1                  | 3.5                                      | 440                   |
| Zirconia (Y-TZP)               | Prozyr      | Norton            | 205                  | 12.0                  | 5.4                                      | 1400                  |
| Alumina-matrix composite (AMC) | DC25        | CeramTec          | 350                  | 19.3                  | 8.5                                      | 1150                  |
| <i>Veneer ceramic</i>          |             |                   |                      |                       |  |                       |
| Porcelain                      | Mark II     | Vita Zahnfabrik   | 68                   | 6.4                   | 0.92                                     | 130                   |
|                                | Empress I   | Ivoclar           | 67                   | 5.6                   | 1.4                                      | 160                   |
| Glass                          | Soda-lime   | Fisher Scientific | 73                   | 5.2                   | 0.67                                     | 110                   |
| <i>Core metal</i>              |             |                   |                      |                       |  |                       |
| Au-alloy                       | Argident 88 | Argen             | 92                   | 1.2                   |  |                       |
| Co-alloy                       | Novarex     | Jeneric/Pentron   | 231                  | 3.0                   |  |                       |
| <i>Substrate</i>               |             |                   |                      |                       |  |                       |
| Polycarbonate                  | Hyzod       | AIN Plastic       | 2.3                  |                       |  |                       |
| Epoxy                          | RT Cure     | Master Bond       | 3.5                  |                       |  |                       |
| <i>Tooth</i>                   |             |                   |                      |                       |  |                       |
| Dental cement                  | Various     |                   | 2–8                  |                       |  |                       |
| Dentin                         |             |                   | 16                   |                       |  |                       |

veneer layer was first fired to each dental ceramic core with fusible glass tape before epoxy-bonding the whole to the substrate, with variable veneer/core thickness ratio but fixed net thickness 1.5 mm. The bonding interlayers were less than 20  $\mu$ m in all cases. Some model all-transparent systems were prepared to highlight the radial crack features in each layer.

Indentations were made on the specimen top surfaces using a tungsten carbide sphere of (cuspal) radius 4 mm, in normal single-cycle loading at a prescribed loading rate. An optical zoom microscope (Optem, Santa Clara, CA) with video tape recorder system provided direct viewing of the specimens during loading. Simultaneous viewing from below the transparent polycarbonate substrate at the ceramic undersurface and through the side walls of any transparent glass layers enabled detection of radial cracks in the core or veneer, respectively. Post-indentation examinations were used to determine critical loads for top-surface fracture (cone cracks) and yield (quasiplasticity<sup>4</sup>) from near-contact stresses [20].

Specific details and statistical analysis of these experiments are covered in earlier publications [24,25]. Extensions of the experimental setup to more complex crown geometries, to metal-core crown systems [15,26],

and to lateral, rotational and multi-cycle loading, are readily accommodated in our setup.

### 3. Results

#### 3.1. Radial crack observations

As indicated, several damage modes can occur in layer structures (Fig. 1). Of these, radial cracking in the ceramic at the lower (cementation) surface is the most deleterious, so we focus on this mode here. Fig. 2 shows side views of typical radial cracks in model all-transparent bilayer [21] and trilayer [27] systems during contact. These model systems use soda-lime glass as the basic “ceramic” layer, with a glass veneer of different modulus in the case of trilayers. The radial cracks form abruptly at a critical load and spread laterally outward over long distances relative to the layer thickness as the load continues to increase. They tend to remain contained within the layer in which they initiate, within the core in the case of trilayers, leaving the crown intact. Contained cracks tend to close up (but not heal) on removal of the indenter and are difficult to detect from *post-indentation* top-surface inspections alone. Subsurface views show that the cracks develop several radial “arms” in a characteristic “star” pattern [21]. At sufficiently high loads the cracks penetrate the entire coating layer and cause catastrophic failure.

<sup>4</sup>Yield in ceramics occurs by a different mechanism to that in metals and usually at a higher contact stress level (higher hardness) than in metals, and is referred to as “quasiplasticity”.

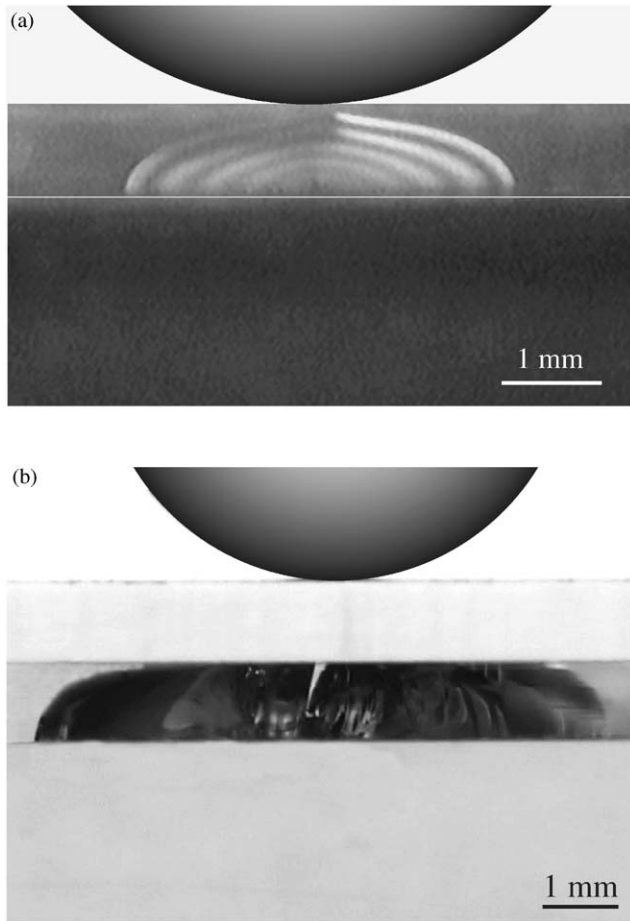


Fig. 2. Side views of radial cracks in all-glass crown-like layer systems in contact with WC sphere: (a) bilayer,  $d = 1$  mm (fringe pattern from light interference at open crack walls), (b) trilayer,  $d_o = d_i = 1$  mm.

### 3.2. Bilayer data

Fig. 3 shows critical loads  $P$  for monolithic plates of Y-TZP (Prozyr), glass-infiltrated alumina and zirconia (InCeram), lithium disilicate glass-ceramic (Empress II) and two porcelains (Empress I and Mark II) bonded to polycarbonate substrates, for indentation with a sphere of radius  $r = 4$  mm at loading rate  $1 \text{ N s}^{-1}$  [24]. Points are experimental data for first observed damage in the ceramic layer, as a function of ceramic thickness  $d$ : at larger  $d$  (unfilled symbols), either cone cracking ( $P_C$ ) or quasiplasticity ( $P_Y$ ), whichever occurs first (quasiplasticity in all cases except Mark II porcelain); at smaller  $d$  (filled symbols), radial cracking ( $P_R$ ). Solid lines are theoretical predictions from corresponding critical load relations [15,22,28–30].

$$P_C = A(T_c^2/E_c)r, \quad (1a)$$

$$P_Y = DH_c(H_c/E_c)^2r^2, \quad (1b)$$

$$P_R = BS_c d^2 / \log(E_c/E_s), \quad (1c)$$

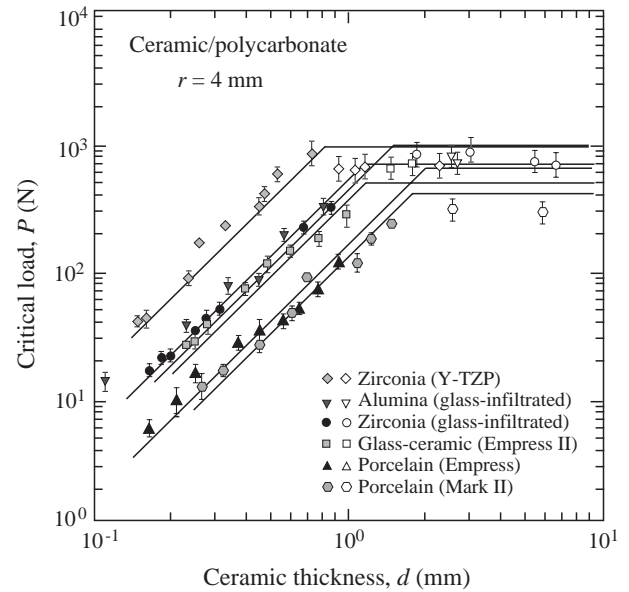


Fig. 3. Critical loads  $P$  for first damage in ceramic/polycarbonate bilayers as a function of ceramic thickness  $d$ , for indentation with WC sphere ( $r = 4$  mm), for a range of dental ceramics [24]. Symbols are experimental data (standard deviation bounds). Solid lines are theoretical predictions for cone cracking or quasiplasticity (horizontal lines) and radial cracking (inclined lines).

where  $E_c$ ,  $T_c$ ,  $H_c$  and  $S_c$  are modulus, toughness, hardness and strength of the ceramic,  $E_s$  is modulus of the substrate, and  $A$ ,  $B$  and  $D$  are dimensionless coefficients. The theory accounts for the main experimental trends. Note that the critical loads are governed primarily by ceramic properties:  $P_C$  by toughness,  $P_Y$  by hardness (or yield stress), and  $P_R$  by strength; elastic modulus  $E_c$  is an additional factor, less important in Eq. (1c). Thus, curves for radial cracking in tougher, harder and (most significantly) stronger materials lie higher in this plot. The radial cracking mode is highly susceptible to the ceramic layer thickness, with quadratic dependence  $P_R \propto d^2$ .

Fig. 4 shows the effect of loading rate on the critical load for radial cracking, for selected ceramics of thickness  $d = 1$  mm on polycarbonate substrates (“dynamic fatigue” tests) [31]. The data are plotted as  $P_R$  versus contact duration  $t$  for radial cracking. The solid lines are fits to the data using standard fracture mechanics relations based on rate-dependent moisture-enhanced growth of the incipient radial cracks [32]

$$P_C = C/t^{1/N}, \quad (2)$$

where  $N$  is a crack velocity exponent and  $C$  is another dimensionless constant. Data extrapolations indicate typical reductions in  $P_R$  of a factor of 2 to 3 over a period of a year or more.

For survival, it is necessary for the load to remain beneath the solid lines in Figs. 3 and 4. Typical occlusal loads are 100–200 N [33], although spikes up to 500 N or

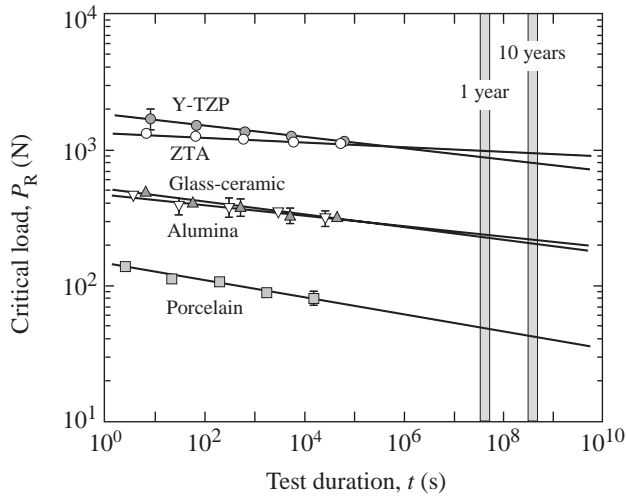


Fig. 4. Critical loads  $P_R$  for radial cracking in ceramic/polycarbonate bilayers as function of test duration  $t$ , for indentation with spheres. Data from constant loading rate tests. Slope of lines is a measure of susceptibility to slow crack growth. Critical loads diminish by a factor or two or more over about a year.

more are possible in extreme cases [14]. On this basis, Y-TZP and AMC are the most resistant to damage initiation, porcelains the least resistant, with InCeram alumina and Empress II intermediate. Such diagrams therefore afford a simple, immediate graphical basis for materials ranking, as well as provide an underlying basis for lifetime prediction. We will return to this element in Section 4.

### 3.3. Trilayer data

Fig. 5 is a plot of the critical load  $P_R$  to produce radial cracks in the inner (i) core ceramic layers fused to outer (o) glass veneer layers and epoxy-bonded to polycarbonate substrates, as a function of glass veneer thickness  $d_o$  (lower axis), or core thickness  $d_i$  (upper axis), for fixed  $d = d_i + d_o = 1.5$  mm (nominal crown thickness). In this case data points are individual experimental results for Y-TZP, alumina and glass-ceramic cores. Solid curves are predictions from a relation derived from conventional elastic plate theory by regarding the outer/inner ceramic duplex as a single ceramic layer of effective modulus  $E_c^*$  [34]

$$P_R = BS_i d^2 (E_c^*/E_i) / \log(E_c^*/E_s) \quad (3)$$

analogous to Eq. (1c), with

$$E_c^* = \frac{E_i \{1 + \varepsilon^2 \delta^3 + \varepsilon \delta (5.66 + 2.18 \delta)\}}{\{1 + 1.97 \delta + \varepsilon \delta [(5.66 - 1.97) + 2.18 \delta + \delta^2]\}}, \quad (4)$$

where  $\varepsilon = E_o/E_i$  and  $\delta = d_o/d_i$ . Again, the solid curves predict the main data trends. Relative to the bilayer limit  $d_i = 1.5$  mm ( $d_o = 0$ ),  $P_R$  diminishes as more of the core is replaced by veneer—aesthetics comes at a cost. Note

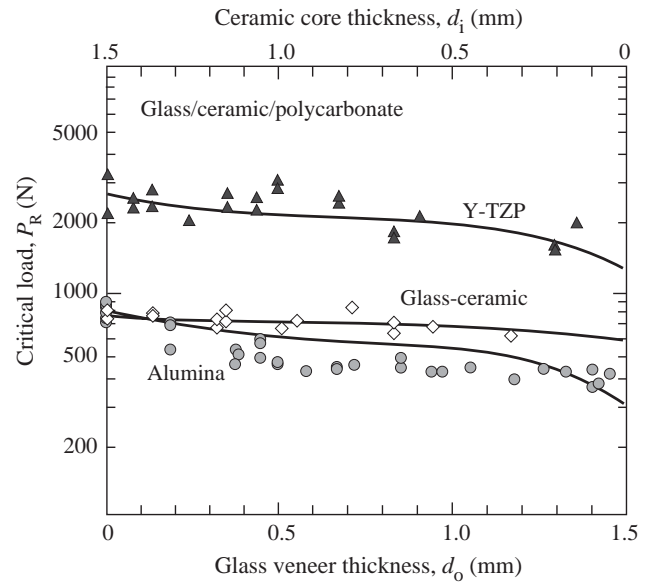


Fig. 5. Critical loads  $P_R$  for inner core radial cracking as function of outer veneer thickness  $d_o$  (or inner thickness  $d_i$ ), for trilayers with common soda-lime glass outer layers and indicated inner core ceramic layers. Results for fixed net thickness  $d = d_o + d_i = 1.5$  mm. Data points are experimental data, solid curves are theoretical predictions.

that the  $P_R$  data plateau out within the region  $d_o = 0.5$  to 1 mm, suggesting that the integrity of the structure is not too sensitive to  $d_o/d_i$  in this intermediate region. Relative modulus  $E_o/E_i$  becomes an important materials factor, along with core strength  $S_i$ .

## 4. Discussion

Experimentation with model layer structures combined with analytical fracture and deformation mechanics provides a sound physical basis for investigating the role of key materials and thickness variables in all-ceramic crown design. Use of flat-layer structures, while simplistic in their representation of crown geometries, enables independent assessment of these key variables. The test protocol can be readily modified step-by-step to include complex occlusal loading, crown geometry and other clinical factors. In its basic form, the test offers immediate insight into critical damage modes in all-ceramic crowns: at the crown top surfaces, cone cracking (leading to tooth chipping) or quasiplasticity (leading to damage accumulation, microcrack coalescence, and accelerated wear); at the crown bottom surfaces, radial cracks (leading ultimately to failure). Clinically, radial cracks are all the more dangerous because they tend to remain subsurface and close up (but, again, not heal) when unloaded, and are thereby difficult to detect by surface inspection alone [22]. Radial cracks are especially dangerous in thin crown structures (Fig. 3) and in prolonged loading (Fig. 4).

A feature of the methodology is the amenability to classical fracture and deformation mechanics, summarized by the relations in Eqs. (1–4). These relations are explicit in their dependence on basic crown thicknesses, and enable some strong conclusions to be drawn. Since  $P_C$  and  $P_Y$  both increase with  $r$ , top-surface damage may be minimized by keeping the crown cuspal radius large enough (by adjusting the opposing dentition to avoid sharp contacts, where possible). More critically, since  $P_R \propto d^2$ , radial cracks can be avoided by keeping the net layer thickness sufficiently large, preferably  $d > 1.5$  mm, within the limits of physiological constraints. A reduction in net crown thickness from  $d = 1.5$  to  $0.5$  mm will result in a corresponding reduction in load  $P_R$  of an order of magnitude. Thus inadvertent thickness reductions in crown preparation and final adjustment should be avoided if at all possible, to avoid the hazardous domain of radial crack domination on the left side of Fig. 3. The simple quadratic  $P_R - d^2$  relationship in Eqs. (3) and (4) is fundamentally based in the theory of flexing plates on soft foundations [22]. On the other hand,  $P_R$  shows a relatively slow dependence on outer/inner thickness ratio  $d_o/d_i$  in trilayers, especially in the intermediate regions (Fig. 5). This inbuilt tolerance in the latter case suggests that relative veneer/core crown thicknesses can be dictated by demands of aesthetics and/or fabrication technologies without adverse effects on structural integrity.

The analytical relations also provide a basis for materials evaluation and ranking. Figs. 3 and 4 show graphically that zirconia (Y-TZP) and alumina-matrix composites (AMC) are the most damage-resistant of the materials studied, porcelains the least resistant, with InCeram alumina and zirconia and Empress II glass-ceramic intermediate. The relative positions of these curves in the thickness domain of radial crack domination are largely determined by the material strengths  $S$  in the  $P_R$  relations. This affirms the appeal of Y-TZP and other ultra-strong materials as crown core materials. To be balanced against this are any potential long-term chemical instabilities, as has been indicated for Y-TZP [2], and any uncommon susceptibility to cyclic fatigue, again as in Y-TZP [35]. Eq. (1b) shows dependence on ceramic hardness [30,34], but this is not so critical provided again the cuspal radius is maintained above a minimum operational level.

Given the critical load relations for trilayers in Eqs. (3) and (4), it is now possible to predict a priori the core fracture response of practical all-ceramic crown-like structures subjected to occlusal loads. It is necessary only to specify appropriate material properties and layer thicknesses. By way of illustration, reduced critical loads  $P_R/P_0$  for porcelain/core-ceramic crowns of fixed net thickness  $d$  and relative thickness  $d_o/d_i = 1$  are plotted in Fig. 6 for selected dental ceramics on a common polymer substrate of nominal mid-range

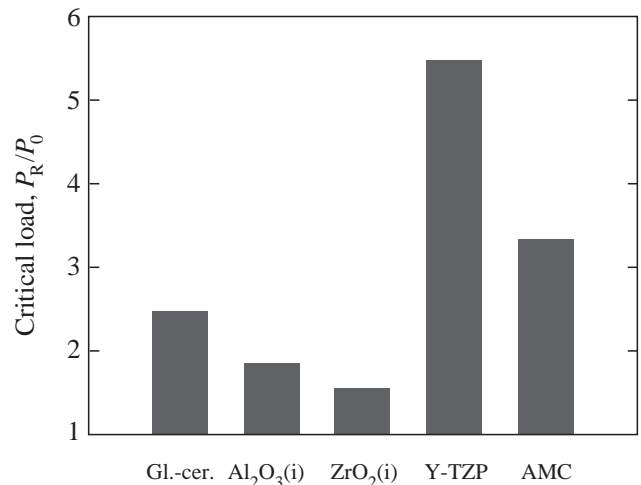


Fig. 6. Bar chart showing predicted critical loads for radial cracking  $P_R$  in ceramic cores with porcelain veneers and dentin substrates in trilayer structures, using materials data from Table 1. Calculations for core thickness  $d_o = d_i$ . Data normalized relative to baseline critical load  $P_0$  for all-porcelain crown; i indicates glass infiltration.

modulus  $E_s = 10$  GPa (effective modulus of a typical composite dental cement layer of  $100 \mu\text{m}$  on dentin base [36]) where  $P_0$  refers to an equivalent all-porcelain crown ( $E_i = E_o = 68$  GPa). The relative positions of the bars in Fig. 6 are determined primarily by strength  $S_i$  and modulus ratio  $E_o/E_i$ . On this basis, some of the ceramics might be considered vulnerable, but Y-TZP and AMC retain their appeal as super-strong materials for future development. Any other potential crown system can be quickly evaluated in this way.

The approach presented here represents just a first step in our attempt to bridge materials science and clinical design. There remain important clinical issues not included in the present analysis—tangential and rotational components of occlusal loading, crown and tooth surface curvature, ceramic surface flaw state (e.g. from machining), presence of voids and defects in the cement, nature of tooth support (natural dentin, buildup, post and core), residual stresses from veneer/core thermal expansion mismatch or from crown/adhesive curing stresses, and so on. One of the most critical outstanding issues is that of fatigue in cyclic loading—typical oral function corresponds to hundreds of thousands of biting cycles per year, in exacting in vivo environments. Fatigue has been studied in some depth for top-surface modes—identified mechanisms include slow growth of cone cracks and (far more deleterious) microcrack coalescence within near-contact quasiplastic zones [35]. Slow crack growth is also manifest in radial fracture, as in the data of Fig. 4. Possible additional modes, near-interface quasiplasticity in softer and tougher ceramic cores and creep in the underlying adhesive/substrate (cement/dentin) complex, are yet to

be systematically studied. These degrading influences, along with inadvertent reductions in crown wall thickness, will tend to lower absolute estimates of  $P_R$ . However, on a relative basis, Fig. 6 remains a useful guide to materials ranking.

Comparative evaluation of crown systems with metal cores has also been carried out in our laboratories, in order to seek answers as to why ceramic systems are relatively vulnerable [26]. In metal-core systems radial cracking occurs preferentially in the veneer rather than the core. Such cracking is generally preceded by yield in the support metal—such yield allows the overlying veneer to flex and thus to develop tension at its undersurface, and is therefore an essential precursor to radial fracture. Yield can also lead to interfacial delamination. The hardness  $H_i$  of the inner core metal then becomes the controlling material property. This conclusion gives credence to McLean's measure of success for all-ceramic crowns, that the strength  $S_i$  of a ceramic core should exceed the yield stress (typically,  $H_i/3$ ) [29] of any comparative core metal. At this time there is no explicit relation to predict the onset of yield in metal-based systems analogous to that for radial fracture in Fig. 1; however, comparative finite element analysis of trilayers with alumina and hard Co-alloy cores (Table 1) indicates similar critical loads for these two systems, suggesting that alumina may be regarded as a “gold standard” for designing the next generation of stronger and longer-lasting all-ceramic crowns [30,34].

## 5. Conclusions

The work described in this article has sought to provide sound physical guidelines for predicting the onset of lifetime-threatening damage in representative biomechanical layer structures. Fundamental relations for competing damage modes (cone cracks, quasiplastic damage, and radial cracks) from occlusal contact in all-ceramic crowns have been experimentally validated. The relations apply across classes of ceramics used for crowns, including porcelains, glass-ceramics, aluminas, and zirconias. Based on these relations, radial fracture, originating from the cementation surface, is a dominant failure mechanism in all-ceramic crowns. Clinically relevant conclusions are:

- (i) The critical load for radial fracture is strongly influenced by net crown thickness ( $P_R$  proportional to  $d^2$ ). A minimum recommended thickness is  $d = 1.5$  mm, in accordance with current dental practice.  $P_R$  is much less dependent on relative veneer/core (outer/inner) ceramic layer thickness, particularly in the region  $d_o/d_i = 1$ , allowing for fabrication tolerance in the dental laboratory.

Prolonged loading can reduce  $P_R$  by a factor of 2 to 3 over a year or more.

- (ii) From the materials standpoint, critical loads are most sensitive to strength  $S$  (ceramics), or hardness  $H$  (metals). This suggests that, perhaps contrary to intuition, a lot more attention should be paid to strengthening the ceramic core material than the porcelain. Modulus  $E$  is also an important factor—stiffer ceramic cores provide more protection to the underlying dentin, but are more susceptible to radial cracking because they support more of the flexural load. For this latter reason, stiff cores are also more vulnerable than veneering porcelains.

## Acknowledgements

This work was supported by a grant from the National Institute of Dental and Craniofacial Research (PO1 DE10976). Specimens were generously supplied by Vita Zahnfabrik, Norton Desmarquest, CeramTec and Ivoclar.

## References

- [1] Kelly JR. Clinically relevant approach to failure testing of all-ceramic restorations. *J Prosthet Dent* 1999;81:652–61.
- [2] Willmann G. Improving bearing surfaces of artificial joints. *Adv Eng Mater* 2001;3:135–41.
- [3] Kelsey WP, Cavel T, Blankenau RJ, Barkmeier WW, Wilwerding TM, Latta MA. 4-Year clinical study of castable ceramic crowns. *Am J Dent* 1995;8:259–62.
- [4] Fradeani M, Aquilano A. Clinical experience with empress crowns. *Int J Prosthodont* 1997;10:241–7.
- [5] Sjogren G, Lantto R, Tillberg A. Clinical evaluation of all-ceramic crowns (Dicor) in general practice. *J Prosthet Dent* 1999;81:277–84.
- [6] Sjogren G, Lantto R, Granberg A, Sundstrom BO, Tillberg A. Clinical examination of Leucite-reinforced glass-ceramic crowns (empress) in general practice: a retrospective study. *Int J Prosthodont* 1999;12:122–8.
- [7] Malament KA, Socransky SS. Survival of Dicor glass-ceramic dental restorations over 14 years: I. survival of Dicor complete coverage restorations and effect of internal surface acid etching, tooth position, gender and age. *J Prosthet Dent* 1999;81:23–32.
- [8] Malament KA, Socransky SS. Survival of Dicor glass-ceramic dental restorations over 14 years: II. Effect of thickness of Dicor material and design of tooth preparation. *J Prosthet Dent* 1999;81:662–7.
- [9] Malament KA, Socransky SS. Survival of Dicor glass-ceramic dental restorations over 16 years: part III. Effect of luting agent and tooth or tooth-substitute core structure. *J Prosthet Dent* 2001;86:511–9.
- [10] McLaren EA, White SN. Survival of in-ceram crowns in a private practice: a prospective clinical trial. *J Prosthet Dent* 2000;83:216–22.

- [11] Fradeani M, Redemagni M. An 11-year clinical evaluation of leucite-reinforced glass-ceramic CROWNS: a retrospective study. *Quintessence Int* 2002;33:503–10.
- [12] Oden A, Andersson M, Krystek-Ondracek I, Magnusson D. Five-year clinical evaluation of procera allceram crowns. *J Prosthet Dent* 1998;80:450–6.
- [13] Thompson JY, Anusavice KJ, Naman A, Morris HF. Fracture surface characterization of clinically failed all-ceramic crowns. *J Dent Res* 1994;73:1824–32.
- [14] Kelly JR. Ceramics in restorative and prosthetic dentistry. *Ann Rev Mater Sci* 1997;27:443–68.
- [15] Zhao H, Hu X, Bush MB, Lawn BR. Cracking of porcelain coatings bonded to metal substrates of different modulus and hardness. *J Mater Res* 2001;16:1471–8.
- [16] McLean JW. The future for dental porcelain. In: McLean JW, editor. *Proceedings of the First international symposium on ceramics*. Chicago: Quintessence Publishing Co; 1983.
- [17] Jung YG, Wuttiaphan S, Peterson IM, Lawn BR. Damage modes in dental layer structures. *J Dent Res* 1999;78:887–97.
- [18] Lawn BR. Indentation of ceramics with spheres: a century after hertz. *J Am Ceram Soc* 1998;81:1977–94.
- [19] Lawn BR, Deng Y, Thompson VP. Use of contact testing in the characterization and design of all-ceramic crown-like layer structures: a review. *J Prosthet Dent* 2001;86:495–510.
- [20] Lawn BR, Deng Y, Miranda P, Pajares A, Chai H, Kim DK. Overview: damage in brittle layer structures from concentrated loads. *J Mater Res* 2002;17:3019–36.
- [21] Chai H, Lawn BR, Wuttiaphan S. Fracture modes in brittle coatings with large interlayer modulus mismatch. *J Mater Res* 1999;14:3805–17.
- [22] Rhee Y-W, Kim H-W, Deng Y, Lawn BR. Contact-induced damage in ceramic coatings on compliant substrates: fracture mechanics and design. *J Am Ceram Soc* 2001;84:1066–72.
- [23] Miranda P, Pajares A, Guiberteau F, Cumbre FL, Lawn BR. Contact fracture of brittle bilayer coatings on soft substrates. *J Mater Res* 2001;16:115–26.
- [24] Deng Y, Lawn BR, Lloyd IK. Characterization of damage modes in dental ceramic bilayer structures. *J Biomed Mater Res (Appl Biomater)* 2002;63:137–45.
- [25] Lawn BR, Deng Y, Lloyd IK, Janal ML, Rekow ED, Thompson VP. Materials design of ceramic-based layer structures for crowns. *J Dent Res* 2002;81:433–8.
- [26] Zhao H, Miranda P, Lawn BR, Hu X. Cracking in ceramic/metal/polymer trilayer systems. *J Mater Res* 2002;17:1102–11.
- [27] Deng Y, Miranda P, Pajares A, Lawn BR. Fracture of ceramic/ceramic/polymer trilayers for biomechanical applications. *J Biomed Mater Res*, in press.
- [28] Lawn BR, Lee KS, Chai H, Pajares A, Kim DK, Wuttiaphan S, et al. Damage-resistant brittle coatings. *Adv Eng Mater* 2000;2:745–8.
- [29] Rhee Y-W, Kim H-W, Deng Y, Lawn BR. Brittle fracture versus quasiplasticity in ceramics: a simple predictive index. *J Am Ceram Soc* 2001;84:561–5.
- [30] Miranda P, Pajares A, Guiberteau F, Deng Y, Lawn BR. Designing damage-resistant brittle-coating structures: I. Bilayers. *Acta Mater* 2003;51:4347–56.
- [31] Zhang Y, Lawn BR. Long-term strength of clinically relevant ceramics. *J Biomed Mater Res*, in press.
- [32] Lee C-S, Kim DK, Sanchez J, Miranda P, Pajares A, Lawn BR. Rate effects in critical loads for radial cracking in ceramic coatings. *J Am Ceram Soc* 2002;85:2019–24.
- [33] DeLong R, Douglas WH. Development of an artificial oral environment for the testing of dental restoratives: Bi-axial force and movement control. *J Dent Res* 1983;62:32–6.
- [34] Miranda P, Pajares A, Guiberteau F, Deng Y, Zhao H, Lawn BR. Designing damage-resistant brittle-coating structures: II. Trilayers. *Acta Mater* 2003;51:4357–65.
- [35] Jung Y-G, Peterson IM, Kim DK, Lawn BR. Lifetime-limiting strength degradation from contact fatigue in dental ceramics. *J Dent Res* 2000;79:722–31.
- [36] Kim JH, Miranda P, Kim DK, Lawn BR. Effect of an adhesive interlayer on the fracture of a brittle coating on a supporting substrate. *J Mater Res* 2003;18:222–7.